ACS OMEGA

Open Access

http://pubs.acs.org/journal/acsodf

Article

Comparison of Seed Morphology and Seed Coat Chemistry in *Ophrys* (Orchidaceae) Species

Erdi Can Aytar,* İsmail Gökhan Deniz, Demet İncedere, Yasemin Özdener Kömpe, Taşkın Basılı, İnes Harzli, and Alper Durmaz

Cite This: *ACS Omega* 2024, 9, 33773−33788

Read Online

ACCESS | Metrics & More | Article Recommendations

ABSTRACT: Orchidaceae is the largest flowering plant family in the world and holds significant importance in terms of biological diversity. Many of the species are found in endemic regions, serving as important indicators for the conservation of biological diversity. Therefore, research on the morphology, seed and embryo structures, chemical composition, and taxonomy of orchids is crucial for species conservation, habitat restoration, and the sustainability of natural habitats. This research involves comparing the morphometric and chemical contents of seeds belonging to certain *Ophrys* L. species and examining interspecies relationships. The micromorphological features of the seeds were analyzed by using light microscopy and scanning electron microscopy (SEM), while their chemical contents were compared by using Fourier transform infrared spectroscopy (FT-IR) analysis. Seed and embryo morphology, morphometric analysis, and seed coat chemistry hold diagnostic significance. In species of the *Ophrys* genus, features like anticlinal wall structure and periclinal wall reticulation are considered weak taxonomic characters. FT-IR analysis identifies specific chemical groups in orchid samples, revealing significant differences in absorbance values and chemical compositions among the different orchid species. Particularly, *Ophrys lycia* (Lycian Kaş Orchid) shows distinct separation from closely related species at peak points such as 2917 and 2850, 1743, 1515, 1240, and 1031 cm^{-1}. Common peak points in the fingerprint region (1200− 700 cm^{-1}) indicate similarity between *O. apifera* and *O. reinholdii* subsp. *reinholdii*. *O. ferrum-equinum*, *O. mammosa* subsp. *mammosa*, *O. fusca* subsp. *leucadica*, *O. reinholdii* subsp. *reinholdii*, and *O. iricolor* exhibit similar absorbance values in the range of 1500−1000 cm^{-1}. These results provide valuable preliminary information about the structure of orchid seed coats, reticulation presence and pattern, chemical profiles, distribution, and dormancy-germination processes.

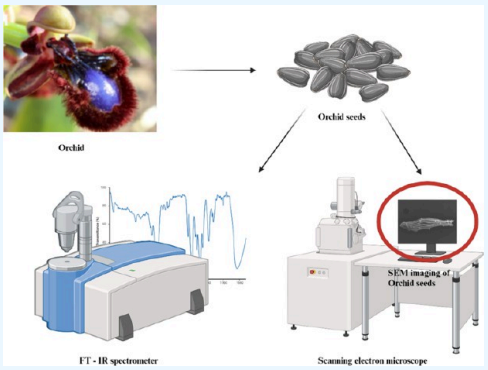

1. INTRODUCTION

Orchids are plants with small and relatively lightweight seeds, and their lengths vary between 100 μm and 1 mm. On average, the seed length ranges from 500 to 900 μm.[1−4] Although the macroscopic appearances of seeds from different genera are similar, their diversity is largely attributed to seed coatings. Mature seeds consist of an undifferentiated, globular embryo enclosed within a transparent and thin seed coat.[5] These seeds lack endosperm, and the occurrence of double fertilization remains uncertain.[6] Numerous studies have shown that seed morphological characteristics can be utilized as taxonomic characters.[1,7−10]

Orchids are found in diverse habitats worldwide, leading to variations in seed germination niches. Seed morphology and seed coat chemical composition provide critical insights into dispersal mechanisms, taxonomy, orchid evolution, and adaptations, as well as the physiological attributes of dormancy and factors responsible for reinitiating embryo growth.[11] Understanding the seed structure, composition, and adaptive traits of endangered orchids will aid in strengthening conservation efforts. Aytar et al.[12] conducted a comprehensive fatty acid analysis in orchid seeds, identifying 30 different compounds. The most abundant fatty acids were linoleic acid (27% in seeds and 33% in tubers) and palmitic acid (24% in flowers). This study highlights both the chemical composition of seeds and the germination processes, offering valuable biological insights for the conservation and propagation of orchid species.

The information regarding the chemistry and function of the seed coat relies on histochemical data obtained using specific dyes. However, these dyes can inadvertently react with other macromolecules, leading to potentially misleading interpreta-

Received: April 1, 2024
Revised: July 12, 2024
Accepted: July 15, 2024
Published: July 24, 2024

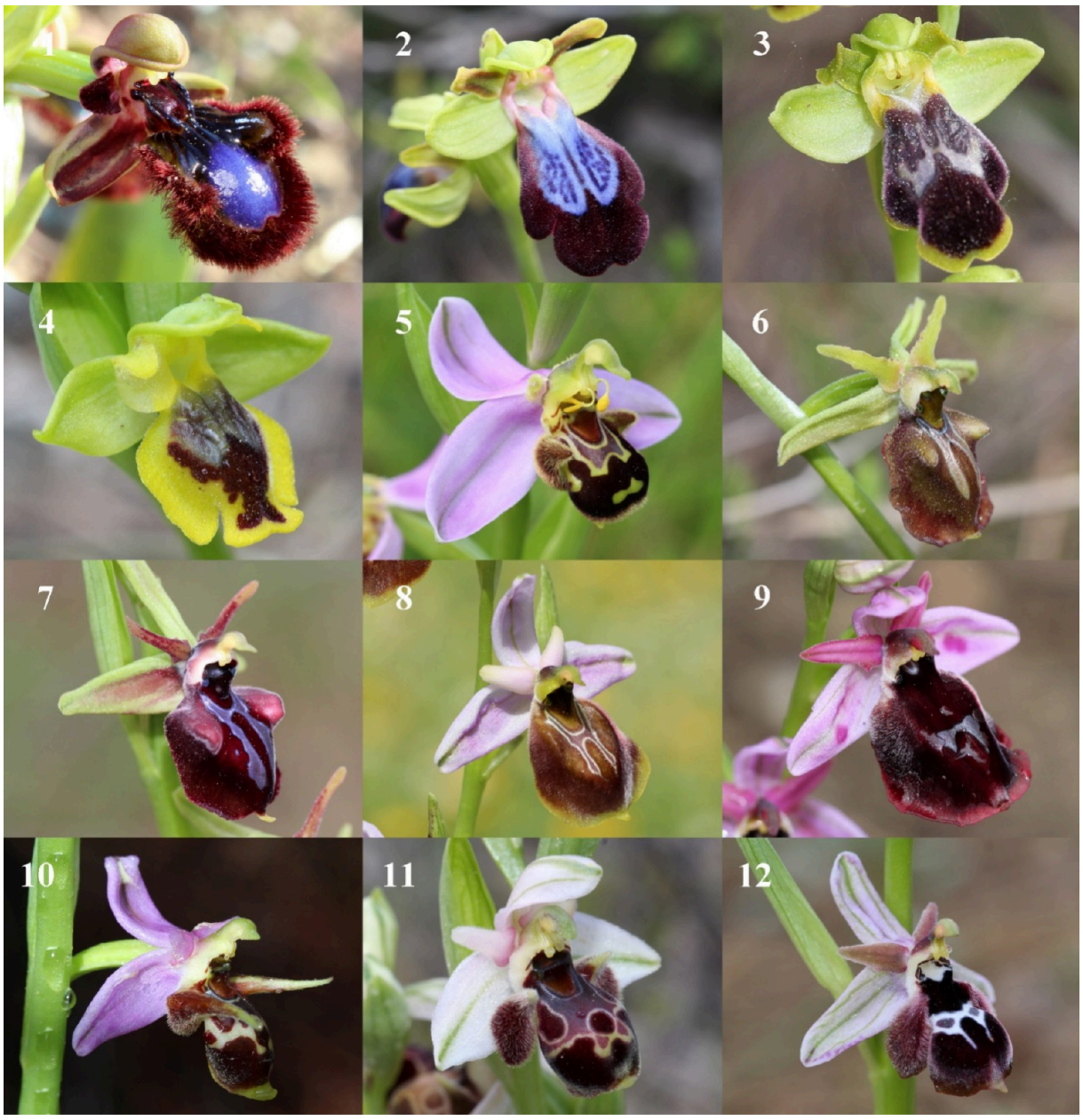

Figure 1. *Ophrys* taxa included in the study: (1) *Ophrys speculum* subsp. *speculum*, (2) *O. iricolor*, (3) *O. fusca* subsp. *leucadica*, (4) *O. lutea* subsp. *galilaea*, (5) *O. apifera*, (6) *O. sphegodes* subsp. herae, (7) *O. mammosa* subsp. *mammosa*, (8) *O. lycia*, (9) *O. ferrum-equinum*, (10) *O. oestrifera* subsp. *oestrifera*, (11) *O. umbilicata* subsp. *umbilicata*, and (12) *O. reinholdii* subsp. *reinholdii* (all photos were taken by Dr. İ. Gökhan Deniz, one of the authors of this study).

tions. For instance, certain lipid dyes can react with phenolic compounds within the tissue.[13,14] Despite the uncertainties of staining techniques, vibrational spectroscopy, in principle, establishes a direct link among vibrational spectrum, band positions, intensities, and molecular structures. Fourier-transform infrared (FTIR) spectroscopy, commonly employed in the chemical analysis of biological materials, offers a rapid and economical means to investigate plant chemical composition.[15] Similar to every individual's fingerprint, the infrared spectrum of any substance is unique. Hence, utilizing infrared spectroscopy enables the identification of unknown samples or the classification of diverse samples.[16] Due to distinct chemical information contained within different orchid species, the FTIR spectroscopy technique can delineate similarities and disparities among orchids. This analytical tool facilitates the identification of major chemical groups and chemical bonds, offering insights into organic and inorganic biochemical compounds found in plants and soil.[17,18] Dogan et al.[19] conducted a comparative analysis of certain plant taxa using FTIR analysis and highlighted that this method provides reliable data for species differentiation. FTIR-ATR (attenuated total reflection) relies on attenuated radiation originating from the surface portion of the sample's spectrum. The penetration depth of ATR varies depending on the wavelength of the refractive index of the utilized crystal and the angle of incidence of the light.[20] Durak et al.[21] investigated the effects of homogeneous plant material preparation and sample measurement methods on the results obtained with ATR-FTIR spectroscopy. The research demonstrated that both sample preparation and measurement methodologies significantly influence the ATR-FTIR spectra.

https://doi.org/10.1021/acsomega.4c03130
ACS Omega 2024, 9, 33773−33788

Additionally, Liu et al.[22] conducted studies revealing differences in plant cell walls using ATR-FTIR spectroscopy.

The assessment of terrestrial temperate orchid seeds encounters limitations with FTIR spectroscopy. The testa layer comprises cell walls, lignins, tannins, lipids, suberins, and polyphenolic deposits. The accumulation of these compounds establishes the testa layer as a significant barrier against water uptake.[23,24] Particularly, the lignification process and other polyphenolic deposits within the testa layer can generate broad and intricate bands in the FTIR spectrum, introducing uncertainties into analyses. Furthermore, in the case of using the FTIR-ATR technique, factors such as the thickness of the testa layer and sample penetration can influence sample analysis.[11] Therefore, the analysis of terrestrial temperate orchid seeds through FTIR spectroscopy may face certain limitations and challenges. Nevertheless, when used in conjunction with other analytical techniques and with the selection of appropriate sample preparation methods, this method is believed to offer valuable insights into the chemical composition of orchid seeds.[25,26]

Ophrys L. (Bee orchids) is a taxonomically challenging genus represented by approximately 45 species ranging from Scandinavia to North Africa, Europe to Iran and Turkmenistan, with the literature containing several hundred taxa.[27−29] While some species have relatively stable character combinations, the majority exhibit extensive morphological diversity. Based on this diversity and morphological variations observed along the distribution range of species, numerous new taxa have been described. While the eighth volume of the Flora of Turkey and the East Aegean Islands lists 27 species of *Ophrys* L., the recent literature has approximately doubled this number with updated information. According to the latest data published in the Illustrated Flora of Turkey, the *Ophrys* genus is represented in Turkey by 29 species (+ 33 subspecies, 3 varieties, 10 hybrid species, 3 hybrid subspecies).[30] The pseudocopulatory mechanism associated with pollinators in the genus and the extensive morphological variation among species pose challenges to classification. While characteristics of sepals and petals are among the distinguishing features at the species level, the most significant distinguishing characters belong to the labelum.

The aim of this study is to compare the morphological characteristics of seeds and the chemical composition of seed coats of *Ophrys* species and to obtain taxonomic and physiological data in addition to morphological distinguishing characters. Sample evaluation is conducted through the analysis of absorbance peaks. Each peak in the spectrum corresponds to a biochemical component, and differences in peak intensities are examined to distinguish between samples. Thus, the importance of FTIR spectroscopy in plant taxonomy and understanding the chemical composition of orchids is highlighted. This method can provide more information about chemical differences among *Ophrys* species and contribute to understanding their taxonomic and evolutionary processes.

2. EXPERIMENTAL SECTION

2.1. Collecting Orchid Seeds and Assessment on Seed Micromorphometric. Seeds of *Ophrys sphegodes* subsp. herae (M.Hirth & H.Spaeth) Kreutz, *Ophrys apifera* Huds., *Ophrys lycia* Renz & Taubenheim, *Ophrys lutea* subsp. *galilaea* (H.Fleischm. & Bornm.) Soó, *Ophrys speculum* subsp. *speculum* Link, *Ophrys iricolor* Desf., and *Ophrys umbilicata* subsp. *umbilicata* Desf., *Ophrys reinholdii* subsp. *reinholdii* Spruner ex Fleischm., *Ophrys fusca* subsp. *leucadica* (Renz) H.Kretzschmar, *Ophrys ferrum-equinum* Desf., *Ophrys mammosa* subsp. *mammosa* Desf., and *Ophrys oestrifera* subsp. *oestrifera* M.Bieb. were collected during the seed maturation period from Samsun, Antalya, and Muğla province (Figure 1). Herbarium records are listed in Table 1. All seeds were obtained through natural pollination in 2018. The seeds extracted from capsules were naturally dried at room temperature for a few weeks and subsequently stored in glass vials in a refrigerator.

Table 1. Herbarium Records Containing *Ophrys* Species

species	herbarium number
Ophrys sphegodes subsp. herae	AKDE-7989
Ophrys apifera	AKDE-8168
Ophrys lycia	AKDE-8078
Ophrys lutea subsp. galilaea	OMUB-8800
Ophrys speculum subsp. *speculum*	OMUB-8801
Ophrys iricolor	OMUB-8799
Ophrys umbilicata subsp. *umbilicata*	AKDE-9005
Ophrys reinholdii subsp. *reinholdii*	AKDE-9822
Ophrys fusca subsp. *leucadica*	AKDE-8156
Ophrys ferrum-equinum	AKDE-9447
Ophrys mammosa subsp. *mammosa*	AKDE-7996
Ophrys oestrifera subsp. *oestrifera*	OMUB-7727

Thirty seeds from each orchid species were measured to determine seed size (length and width) and embryo size (length and width) using a modified light microscope (DM4000 B; Leica), a motorized specimen stage for automatic sampling (Bio Precision MAC 5000 controller system; Ludl Electronic Products. Hawthorne. NY), and a CCD color video camera (Optronics Micro Fire. Goleta. CA).

Seed, embryo, and air space volume were calculated as follows as described by[31]

$$\text{embryo volume: Ev} = (4/3) \times (22/7) \times (\text{EL}/2) \times (\text{EW}/2)^2 \quad (1)$$

$$\text{seed volume: Sv} = 2 \times ((\text{SW}/2)^2 \times (\text{SL}/2) \times (1.047)) \quad (2)$$

$$\text{air} - \text{space volume: ASV} = (\text{SV} - \text{EV} \times 100)/\text{Sv} \quad (3)$$

where SW is the seed width, SL is the seed length, EW is the embryo width, and EL is the embryo length.

2.2. Scanning Electron Microscope Imaging. The dry seeds were carefully dissected and then mounted onto stubs using double-sided carbon tape for electron microscopy imaging. To enhance conductivity and provide a better imaging surface, the samples were coated with a thin layer of gold−palladium (12.5−15 nm) using an SEM coating system (SC7620). The examination and imaging processes were conducted using a JEOL JMS-7001F scanning electron microscope (SEM) at a voltage range of 5−15 kV.[32] Various aspects such as seed shape, seed coat reticulating, and cell wall edge structure were thoroughly evaluated and analyzed based on the obtained SEM electron micrographs.

2.3. FT-IR Analysis of Seed Coats. The embryos and inner seed coats were removed with a needle using a stereomicroscope. No chemical treatment was applied and allowed only the outer seed coat surface analysis. Attenuated total reflection-Fourier transform infrared (ATR-FTIR) analyses were performed using a Spectrum 400 spectrophotometer (PerkinElmer, Waltham, MA, USA) equipped with a DTGS

https://doi.org/10.1021/acsomega.4c03130
ACS Omega 2024, 9, 33773−33788

Table 2. Principal Seed Characters of the 12 *Ophrys* Species

species name	seed color	seed shape	cell number on longitudinal axis	differences between chalazal and medial region cell	reticulation of periclinal cell wall
Ophrys sphegodes subsp. herae	light brown	fusiform	4−6	absent	straight/anastomosed
Ophrys apifera	yellowish brown	fusiform	5−7	present	straight/anastomosed
Ophrys lycia	yellowish brown	fusiform	4−6	present	straight/anastomosed
Ophrys lutea subsp. *galilaea*	dark brown	clavate	4−6	present	straight/anastomosed
Ophrys speculum subsp. *speculum*	dark brown	clavate	5−7	present	straight/anastomosed
Ophrys iricolor	dark brown	fusiform	4−6	present	inclined/anastomosed
Ophrys umbilicata subsp. *umbilicata*	light brown	fusiform	3−6	present	straight/anastomosed
Ophrys reinholdii subsp. *reinholdii*	light brown	clavate	4−6	present	straight, inclined anastomosed
Ophrys fusca subsp. *leucadica*	brown	fusiform	4−6	present	straight/anastomosed
Ophrys ferrum-equinum	light brown	clavate	4−5	present	inclined/anastomosed
Ophrys mammosa subsp. *mammosa*	light brown	fusiform	5−7	present	straight/anastomosed
Ophrys oestrifera subsp. *oestrifera*	dark brown	clavate	4−5	present	straight/anastomosed

(deuterated triglycine sulfate) detector. In general, a scan/spectrum was obtained with a resolution of 4 cm^{-1} in the range of 4000−400 cm^{-1}.[11] Samples were analyzed without any prior processing. Peak frequencies were determined by using the PerkinElmer Spectrum One FTIR software. Secondary peaks and absorbance values determined and calculated with the PerkinElmer Spectrum Quant Program)

2.4. Statistical Analysis. In this research, the use of ANOVA and Duncan tests is crucial for understanding the statistical analysis of micromorphological differences among seeds. The ANOVA (analysis of variance) test was employed to assess whether there are statistically significant differences in seed features among the various species. This test is particularly useful when comparing the means of three or more groups, as it helps determine if at least one group's mean is different from the others. The importance of using ANOVA lies in its ability to handle multiple groups simultaneously, thus providing a comprehensive overview of the data's variance and ensuring that any observed differences are not due to random chance.

After establishing that there are significant differences with the ANOVA test, the Duncan test was used as a pairwise post-hoc test to pinpoint exactly which species' seed features differ from each other. The Duncan test helps to identify specific pairs of groups that have significant differences in their means. This test is particularly valuable because it controls for type I errors (false positives) when making multiple comparisons, thus providing more precise results regarding interspecies differences.

Both tests were conducted using the SPSS package program for Windows (version 21),[33] which is a widely used statistical software that facilitates robust data analysis through user-friendly interfaces and advanced statistical functions. This combination of ANOVA and the Duncan test ensures a thorough and accurate analysis of the micromorphological differences among seeds, making the results reliable and meaningful for further interpretation and application.

FTIR peak intensity and area were measured using the OMNIC software after spectra normalization. Statistics and curve fitting were done using the Origin software.[34]

For the graphical representation of seed dimensions and FTIR analysis results with species-specific clustering. Principal component analysis (PCA) was conducted using Past program Version 4.03.

3. RESULTS AND DISCUSSION

3.1. Seed Micromorphological Evaluation. In the taxonomic differentiation of the *Ophrys* genus, the sizes of the floral parts are significant distinguishing features among generative characters. Species and their close relatives are evaluated within groups based on characteristics such as the number and shape of lip divisions, color, presence of shoulders, pattern shape, structure of the connective, and whether there is additional appendage at the tip of the lip. Within the same group, flower tissue colors are as prominent as sizes among species. Typically, reaching a conclusion on species diagnosis is achieved by the presence of characteristics such as the posture and size of sepals and petals, petal shape and indumentum, type of indumentum on the outer edges of the lip, and the number of flowers, supporting these characters.[30] The diversity in relevant morphological characteristics within the genus is so extensive that, along with the formation of hybrid individuals among species through pollination mechanisms, taxonomy has become almost intricate in recent times. One of the most influential factors in this complexity is the publication of individuals with characteristics within the morphological boundaries of taxa from one region to another as new taxa in the scientific world. Researchers evaluating species within groups can classify this group under a single species name with a holistic approach, while they can also divide it into dozens of taxa, each indicating a new name and taxon, even with the slightest variation in character. For these reasons, effective distinctions and a holistic approach to new characters that can be used in the taxonomy of the genus are needed.

In this study on the seed morphology and seed coat chemistry of the genus, the focus has been on the differences in the smallest units that perpetuate the species. According to SEM micrographs, the structure of the anticlinal and periclinal walls of seed coat cells can be considered to have weak taxonomic character within the *Ophrys* genus. However, previous studies have considered it a relatively significant character among different genera or species within the same genus.[2,8,9]

https://doi.org/10.1021/acsomega.4c03130
ACS Omega 2024, 9, 33773−33788

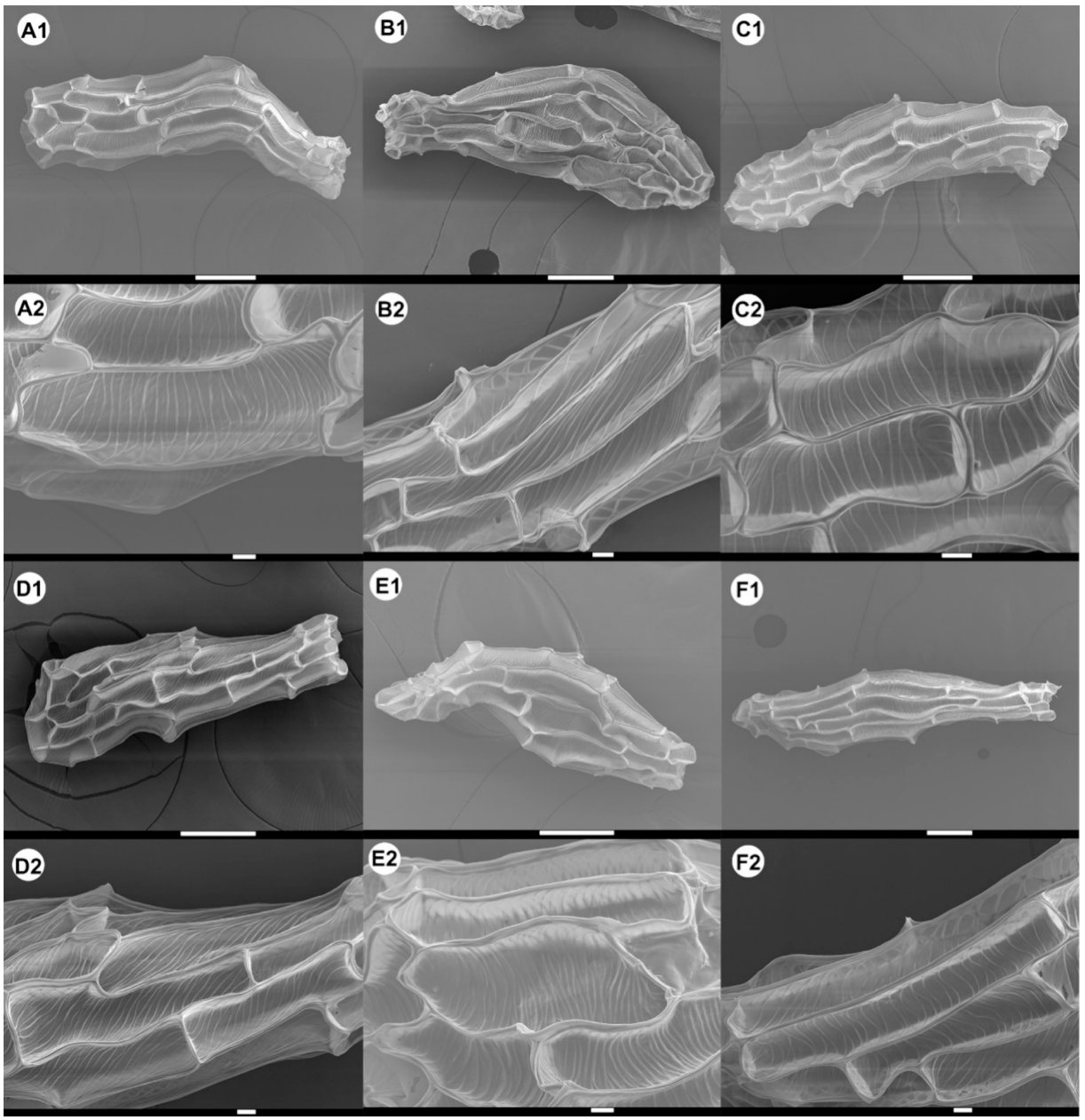

Figure 2. SEM images of seeds and testa cells are as follows: (A1) General seed image *O. apifera*, (A2) Testa cell image of *O. apifera*, (B) *O. ferrum-equinum*, (C) *O. fusca* subsp. *leucadica*, (D) *O. iricolor*, (E) *O. lutea* subsp. *Galilaea*, (F) *O. lycia*. The scale bar for general seed images (A1, B1, C1, D1, E1, F1) is 100 μm and for testa cell images (A2, B2, C2, D2, E2, F2) is 10 μm.

The anticlinal wall structure in the seed coat, presence and orientation (vertical/inclined) of reticulation in the periclinal walls, and the presence of anastomosis in the reticulation were evaluated based on SEM images and are presented in Table 2. The presence of reticulation in the periclinal cell walls of all *Ophrys* species studied was observed in the SEM images. In seeds of *O. ferrum-equinum* and *O. iricolor*, periclinal cell walls were inclined, reticulated, and anastomosed, whereas in *O. reinholdii* subsp. *reinholdii*, both vertical and inclined reticulated and anastomosed cells were notable. In species other than these three, the reticulation is vertical and anastomosed. The anticlinal cell walls of seeds belonging to all species are flat.

The examined species exhibited a range of variations in seed shape, spanning from fusiform to clavate. In certain species with fusiform-shaped seeds, the central region displayed greater width than the ends due to the embryo's positioning. Variations were observed in several characteristics of the anticlinal walls of the chalazal pole cells, with the basal cells appearing short and polygonal, while the medial cells were elongated (Figures 2 and 3).

The conducted one-way analysis of variance (ANOVA) revealed significant variations in the morphological data of the measured seeds among the 12 studied species. To determine the specific changes among species groups with significant differences, Duncan's test was applied, and the results are presented in Table 3.

Seed length significantly varied based on species (F (11, 348) = 51.563, p = 0.000). The longest seeds were found in *O. apifera*, whereas the smallest seed length was observed in *O. umbilicata* subsp. *umbilicata*. Seed width also showed significant differences based on species (F (11, 348) = 27.046, p = 0.000). The widest seeds were in *O. apifera*, while the narrowest seeds were in *O.*

https://doi.org/10.1021/acsomega.4c03130
ACS Omega 2024, 9, 33773−33788

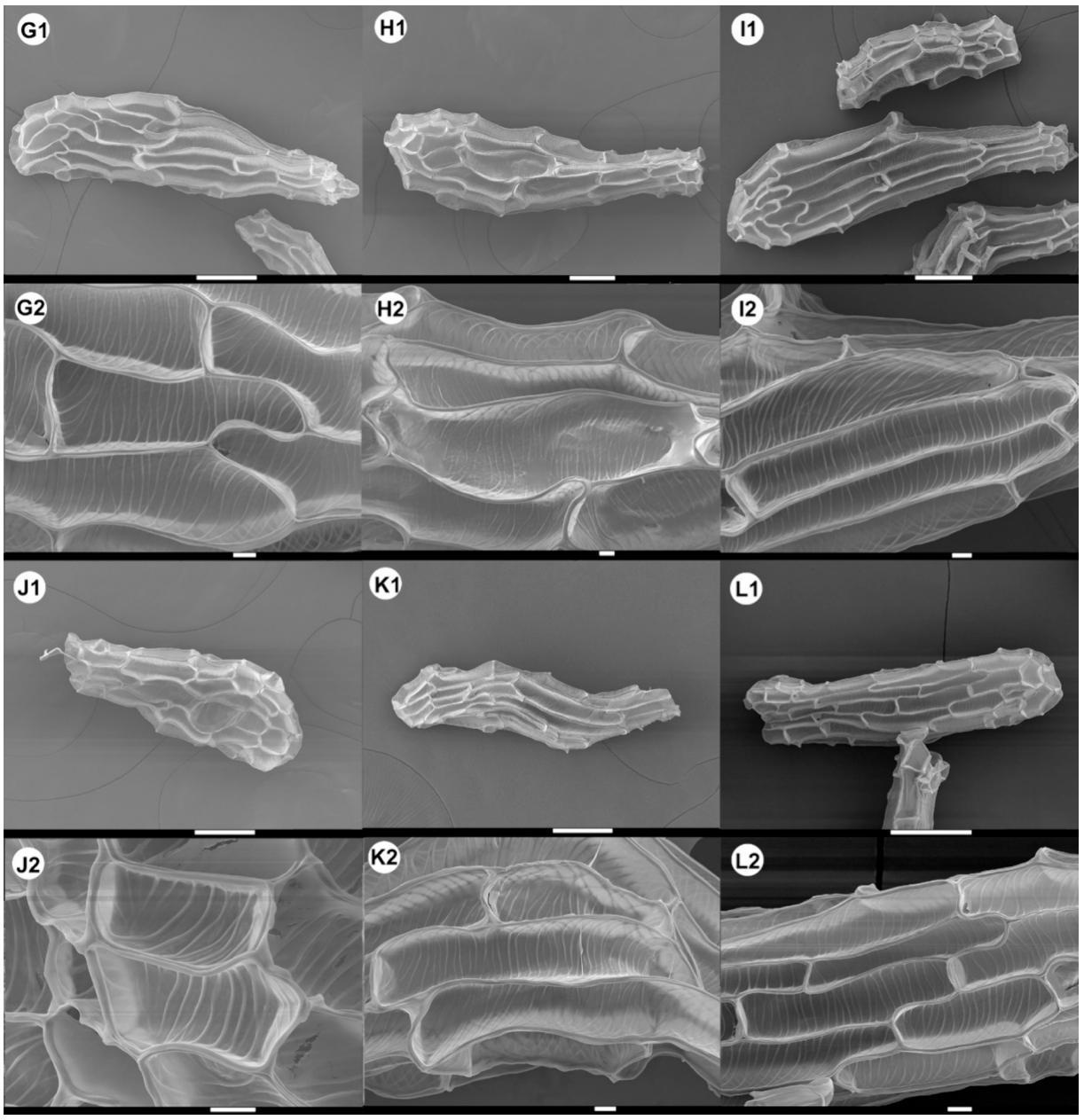

Figure 3. SEM images of seeds and testa cells are as follows: (G1) General seed image *O. mammosa* subsp. *mammosa*, (G2) Testa cell image of *O. mammosa* subsp. *mammosa*, (H) *O. oestrifera* subsp. *oestrifera*, (I) *O. reinholdii* subsp. *reinholdii*, (J) *O. speculum* subsp. *speculum*, (K) *O. sphegodes* subsp. *herae*, and (L) *O. umbilicata* subsp. *umbilicata*. The scale bar for general seed images (G1, H1, I1, J1, K1, and L1) is 100 μm, and for testa cell images (G2, H2, I2, J2, K2, and L2) it is 10 μm.

umbilicata subsp. *umbilicata*. The seed length/width ratio exhibited significant variations among species (F (11, 348) = 6.624, p = 0.000). The largest seed length/width ratio was measured in *O. reinholdii* subsp. *reinholdii*, while the smallest ratio was in *O. lutea* subsp. *galilaea*.

Regarding seed volume values, there were significant differences based on species (F (11, 348) = 38.483, p = 0.000). *O. speculum* subsp. *speculum* had the largest seed volume, whereas *O. umbilicata* subsp. *umbilicata* possessed the smallest seed volume. In terms of embryo morphological assessment, the embryo length significantly varied among species (F (11, 348) = 44.255, p = 0.000). The species with the longest embryo was *O. apifera*, whereas the shortest embryo was observed in *O. umbilicata* subsp. *umbilicata*. Embryo width also showed significant differences based on species (F (11, 348) = 37.948, p = 0.000). The narrowest embryo belonged to *O. umbilicata* subsp. *umbilicata*, while the widest embryo was found in *O. apifera*.

Upon analyzing the embryo length/width ratio, significant changes were detected among species (F (11, 348) = 2.535, p = 0.004). The species with the highest ratio was *O. oestrifera* subsp. *oestrifera*, and the lowest ratio was observed in *O. lycia*. Concerning embryo volume, significant differences were found among species (F (11, 348) = 45.953, p = 0.000). When comparing species, *O. umbilicata* subsp. *umbilicata* had the lowest embryo volume, while *O. apifera* had the highest volume. The analysis of the seed volume/embryo volume ratio revealed significant changes in measurements among species (F (11, 348) = 34.401, p = 0.000). The species with the highest volume ratio was *O. speculum* subsp. *speculum*, whereas the lowest ratio was

https://doi.org/10.1021/acsomega.4c03130
ACS Omega 2024, 9, 33773−33788

Table 3. Comparative Measurement of Seed Micromorphological Characteristics of 12 Selected *Ophrys* Species and Post-hoc (Duncan) Comparisons after ANOVA[a]

species name	seed length	seed width	seed length/width	seed volume	embryo length	embryo width	embryo length/width	embryo volume	seed volume/embryo volume	vacancy percentage
Ophrys sphegodes subsp. herae	0.481 ± 0.070 cd	0.119 ± 0.019 d	4.10 ± 0.76 bcd	1.88 ± 0.73 d	0.129 ± 0.017 de	0.082 ± 0.015 c	1.61 ± 0.38 ab	0.47 ± 0.19 d	4.26 ± 1.72 cd	72.14 ± 13.35 cde
Ophrys apifera	0.625 ± 0.079 a	0.169 ± 0.026 a	3.76 ± 0.66 cde	4.84 ± 1.81 a	0.186 ± 0.033 a	0.119 ± 0.019 a	1.58 ± 0.32 ab	1.45 ± 0.59 a	3.78 ± 1.82 cd	67.68 ± 14.45 de
Ophrys lycia	0.584 ± 0.135 b	0.134 ± 0.024 c	4.48 ± 1.33 ab	2.83 ± 1.14 bc	0.133 ± 0.027 cd	0.100 ± 0.015 b	1.33 ± 0.23 c	0.75 ± 0.32 c	4.23 ± 2.02 cd	71.93 ± 11.09 cde
Ophrys lutea subsp. *galilaea*	0.362 ± 0.060 e	0.115 ± 0.022 d	3.21 ± 0.71 f	1.33 ± 0.63 de	0.114 ± 0.018 fg	0.072 ± 0.015 de	1.66 ± 0.50 ab	0.33 ± 0.15 def	1.00 ± 0.52 e	74.25 ± 8.29 cd
Ophrys speculum subsp. *speculum*	0.367 ± 0.050 e	0.111 ± 0.023 de	3.40 ± 0.68 ef	5.06 ± 2.72 a	0.116 ± 0.017 efg	0.073 ± 0.011 de	1.60 ± 0.24 ab	0.34 ± 0.13 def	15.82 ± 8.36 a	92.23 ± 3.32 a
Ophrys iricolor	0.350 ± 0.076 e	0.099 ± 0.021 ef	3.61 ± 0.91 def	0.97 ± 0.47e	0.106 ± 0.022 fh	0.066 ± 0.017 ef	1.67 ± 0.42 ab	0.27 ± 0.15 def	4.19 ± 1.88 cd	71.31 ± 12.54 cde
Ophrys umbilicata subsp. *umbilicata*	0.339 ± 0.040 e	0.092 ± 0.022 f	3.85 ± 0.94 cde	0.82 ± 0.48 de	0.094 ± 0.015 h	0.060 ± 0.010 f	1.61 ± 0.40 ab	0.18 ± 0.07 f	4.92 ± 4.14 c	72.43 ± 12.40 cde
Ophrys reinholdii subsp. *reinholdii*	0.463 ± 0.070 d	0.103 ± 0.022 ef	4.71 ± 1.21 a	1.36 ± 0.64 e	0.119 ± 0.022 ef	0.077 ± 0.017 cd	1.61 ± 0.43 ab	0.40 ± 0.22 de	4.03 ± 2.93 cd	66.94 ± 16.98 e
Ophrys fusca subsp. *leucadica*	0.509 ± 0.064 c	0.148 ± 0.027 b	3.53 ± 0.78 ef	3.05 ± 1.23 bc	0.145 ± 0.024 bc	0.102 ± 0.021 b	1.48 ± 0.37 bc	0.84 ± 0.41 c	4.04 ± 1.68 cd	71.37 ± 10.63 cde
Ophrys ferrum-equinum	0.464 ± 0.074 d	0.118 ± 0.028 d	4.15 ± 1.31 bcd	1.81 ± 0.93 d	0.112 ± 0.021 fg	0.067 ± 0.012 ef	1.72 ± 0.50 a	0.28 ± 0.12 def	6.85 ± 3.21 b	81.51 ± 9.50 b
Ophrys mammosa subsp. *mammosa*	0.588 ± 0.083 ab	0.145 ± 0.024 bc	4.16 ± 0.96 bcd	3.32 ± 1.24 b	0.148 ± 0.026 b	0.096 ± 0.016 b	1.58 ± 0.36 ab	0.74 ± 0.29 c	5.26 ± 3.83 bc	75.72 ± 9.79 bc
Ophrys oestrifera subsp. *oestrifera*	0.550 ± 0.079 b	0.134 ± 0.021 c	4.22 ± 1.01 abc	2.62 ± 0.87 c	0.180 ± 0.029 a	0.104 ± 0.022 b	1.80 ± 0.47 a	1.08 ± 0.52 b	2.78 ± 1.18 cd	57.84 ± 16.66 f

[a]All measurements are in micrometers (μm).

https://doi.org/10.1021/acsomega.4c03130
ACS Omega 2024, 9, 33773−33788

Table 4. Loadings of Seed Morphological Data on PC1 and PC2

	seed morphological data	
	positive loadings	negative loadings
PC1	the percentage of gap, seed volume/embryo volume, seed volume	embryo width, seed width, seed length, embryo length/width ratio (L/W), embryo length, embryo volume, seed length/width ratio (L/W)
PC2	seed volume/embryo volume, seed volume, embryo volume, seed length/width ratio (L/W), seed length, embryo length, embryo width, embryo length/width ratio (L/W), seed width	the percentage of gap

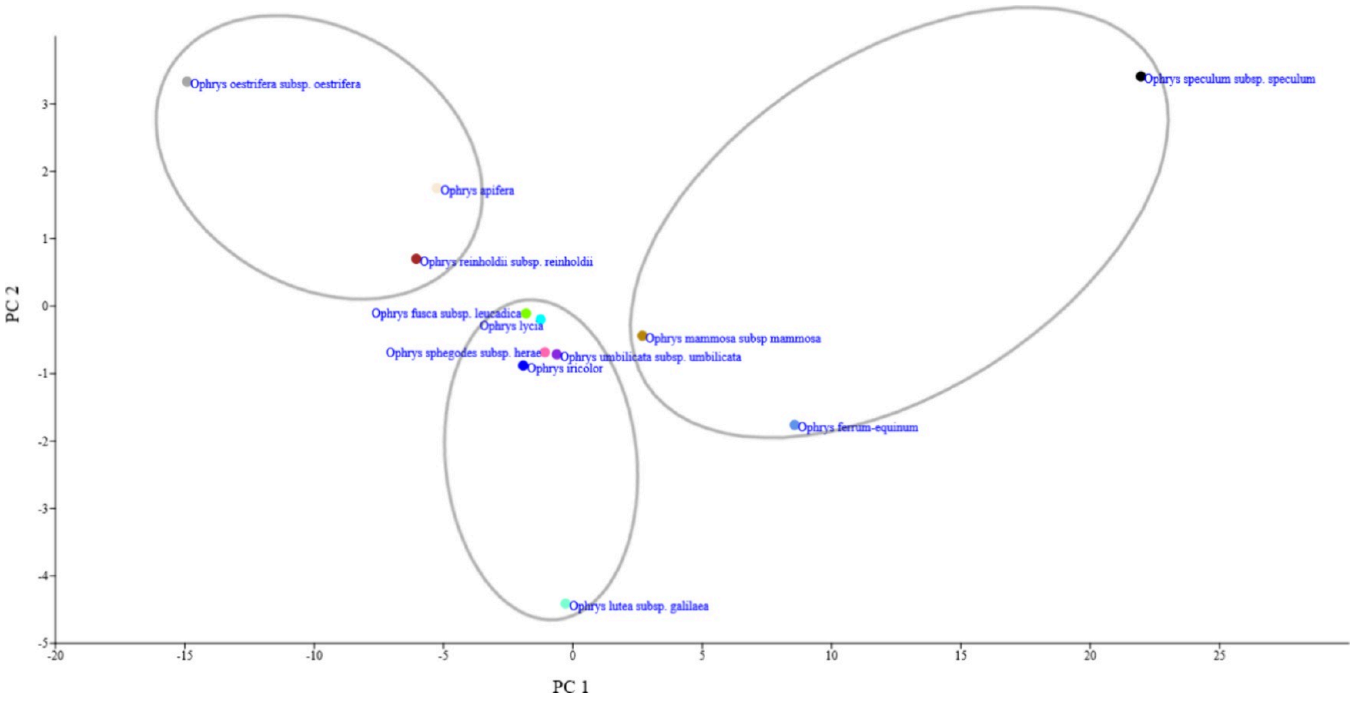

Figure 4. PCA plot illustrating the species-dependent variations in seed measurements.

observed in *O. lutea* subsp. *galilaea*. Lastly, considering the void percentage, significant differences were observed among species ($F(11, 348) = 13.966$, $p = 0.000$). *O. speculum* subsp. *speculum* exhibited the highest void percentage, while the lowest void percentage was found in *O. oestrifera* subsp. *oestrifera*.

When the morphological measurements of the obtained seeds are compared with various studies in the literature containing similar measurements, it is found that the seed measurements of the species are similar to those in some studies in the literature, while they differ from others. Indeed, it is observed that different studies of the same species in the literature also yield different results. For instance, in Aybeke,[9] the measurements of *O. sphegodes* and *O. apifera* seeds indicate smaller seeds compared to our findings, while it was determined that our measurements for *O. mammosa* and *O. oestrifera* are similar to each other. Similarly, in another study, while the measurements of *O. lutea* seeds correspond to our findings, the measurements of *O. speculum* and *O. iricolor* seeds Deniz et.[29] are smaller than our measurements. In another study, the measurements of *O. fusca*, *O. speculum*, and *O. sphegodes* seeds match our measurements; however, while our measurements for *O. apifera* seeds are higher than the measurements in this study, it was observed that our measurements for *O. lutea* seeds[35] are lower. We believe that the differences may be attributed to variations in the time of seed collection, maturity status of the seeds, ecological differences in the areas where the plants were collected, and the precision of the measurements taken.

3.2. PCA Results. Principal component analysis (PCA) is a statistical technique used to reduce the dimensionality of multivariate data and identify the primary variables (principal components). PCA creates new variables (principal components) that maximize the variance in the data, making it easier to visualize patterns and relationships within the data sets. PCA is particularly effective for understanding and interpreting data sets with high correlations among the variables.[36] According to the results of PCA, orchid species located within the same ellipse possess seed characteristics more similar to those of other species. *O. speculum* subsp. *speculum*, *O. mammosa* subsp. *mammosa*, and *O. ferrum-equinum* have shown distinct positioning from other species due to their similar seed characteristics and have been clustered on the positive side of the PC1 axis. Although the remaining species are located on the negative side of the PC1 axis, considering the PC2 axis, *O. oestrifera* subsp. *oestrifera*, *O. apifera*, and *O. reinholdii* subsp. *reinholdii* are clustered on the positive part of the axis, while other species are grouped on the negative part of the PC2 axis. PC1 explains 92.8% of the total variance in the quantitative data followed by PC2 with 5.4%, resulting in a cumulative variance of 98.2% (Table 4, Figure 4). The key quantitative characteristics contributing to the formation of observed clusters in PCA were percentage of gap, seed volume/embryo volume, and seed volume. Additionally, significant quantitative characteristics in this study included embryo width, seed width, seed length, embryo length/width ratio (L/W), embryo length, embryo

https://doi.org/10.1021/acsomega.4c03130
ACS Omega 2024, 9, 33773−33788

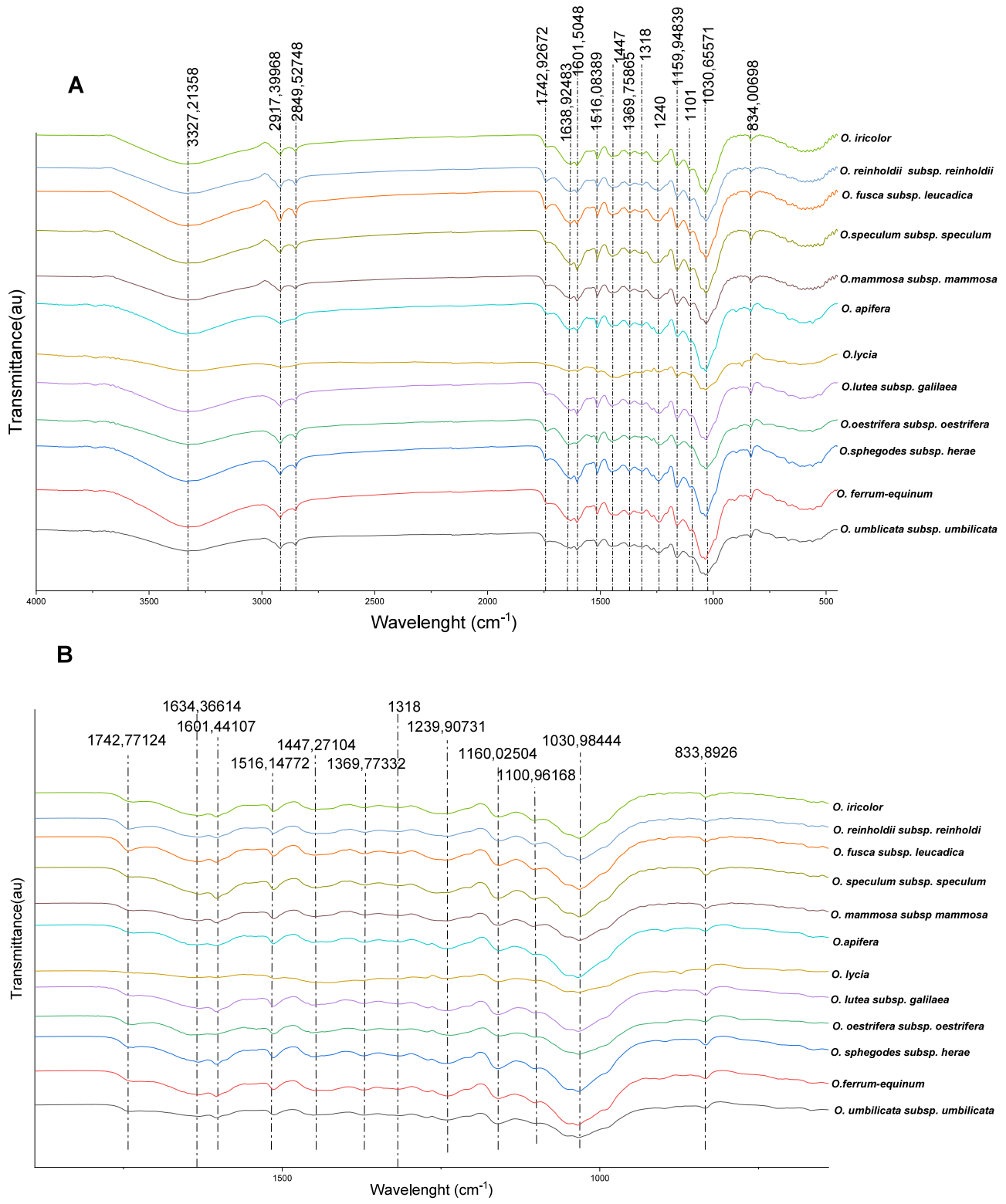

Figure 5. (A) Spectra of all analyzed *Ophrys* species in the range of 4000−400 cm^{-1} and (B) expended spectra of all analyzed *Ophrys* species in the range of 1800−400 cm^{-1}.

volume, and seed length/width ratio (L/W). The contributions of the measured variables to PCA are presented in the table below.

The main characteristics providing the initial differentiation in terms of morphological variation are observed to be the volume of seeds, percentage of void space, seed volume/embryo volume ratio, and length/width ratio. When evaluated in this aspect, it is noteworthy that *O. speculum*, which is located in the first separated group and has extreme positive values in both PC1 and PC2 correlations, is considered the most primitive species in terms of morphological development. The presence of a bright blue pattern resembling a mirror spread across the entire surface

https://doi.org/10.1021/acsomega.4c03130
ACS Omega 2024, 9, 33773−33788

Table 5. Characteristic FT-IR Bands of *Ophrys* Seed Coats

wavenumber (cm^{-1})	chemical assignment	source
3600−3100	O−H and C−H stretching vibration	polysaccharides
3329	O−H stretching vibration (Hydrogen bonded)	cellulose and lignin
2917 and 2850	-CH_2 stretching vibrations (aromatic methoxy groups and methylene and methyl groups)	polysaccharides, lipids, and lignin
1743	C═O stretching vibration of carboxyl and acetyl group	hemicellulose
1601	aromatic skeleton vibration	lignin
1516	COO- stretching	hemicellulose
1443	C−H plane deformation	cellulose
1371	asymmetric CH_2 bending	cellulose and lignin
1318	CH_2 wagging	cellulose and lignin
1239	in plane OH bending	cellulose and lignin
1155	C−O stretching of ester groups	cellulose and hemicellulose
1102	aromatic C−H deformation of syrgnl units	lignin
1030	O−H stretching of primary alcohols	polysaccharides, cellulose, and lignin
833	C−H out of plane deformation	lignin

of the labelum and long soft hairs on the lip edges in the flowers of this species places it in a morphologically isolated position with characters not seen in any other *Ophrys* species on the Earth.[29] It is quite intriguing that the same isolative conditions are observed in the seeds of the species. Indeed, *O. speculum*, considered the most primitive species morphologically within the *Ophrys* species of the Mediterranean region and having the widest distribution range among all species, also possesses the largest seeds. The species has the most extreme values within the study, with a seed volume of 5.06 μm, the highest seed volume/embryo volume ratio of 15.82 (with a moderately sized embryo dimensions of 0.34), and a void space percentage of 92.23. When evaluated in this aspect, a gradual decrease in the seed size can be observed with increasing development. Another data supporting this view is observed in *O. apifera*, with PC1 having positive and PC2 having negative values. Considering the morphological features of the taxa within the scope of the study, according to the Illustrated Flora of Türkiye, *O. apifera*, which has attached lip tips and pointed connectives, is the most primitive species of the groups with attached lip tips and pointed connectives (excluding *O. speculum* and *O. fusca* group species).[30] Interestingly, after *O. speculum*, the largest seeds in terms of the relevant numerical values belong to *O. apifera*. In all subsequent species, a gradual decrease in the seed size is observed with increasing development.

The emerginate shape of the labelum at the tip and its lack of appendage, the fragmented form of the labelum with three lobes at the edges, and the blunt shape of the connective at the tip bring *O. speculum*, the most primitive species in the study, morphologically closer to the species in the *O. fusca* group.[30] *O. fusca* ssp. *leucadica*, *O. lutea* ssp. *galilea*, and *O. iricolor*, included in the study, are species within this group and exhibit all three main characters prominently. The fact that all three taxa are placed in the same group in the PCA obtained from studies of seed morphology supports this character integrity. Among these species, *O. fusca* is interpreted to carry more ancestral characters. In addition to a similar pattern structure, the yellow and wing-like bands formed at the edges and tip of the labelum indicate a more developed morphology. As corroborated, the taxon with the smallest volume values for both seed and embryo is identified as *O. lutea* ssp. *galilea*

Another pair of species that are morphologically brought closer together by seed morphological measurements within the genus is *O. mammosa* and *O. ferrum-equinum*. Scientific names such as *O. mammosa*, *O. ferrum-equinum*, *O. argolica*, and closely related taxa have often been subject to taxonomic transfers among each other. Essentially, the shoulder structure seen in *O. mammosa*, the pattern spread across the entire labelum in the shape of the letter H, and the brownish lip character are not observed in the other two species. This morphological difference has also supported the separation of *O. mammosa* from *O. ferrum-equinum* in terms of seed morphology evaluated in this study. These two species are close enough to be placed in the same group in PCA yet sufficiently distant to highlight their differences. A similar difference to *O. mammosa* is observed in *O. sphegodes*. According to some taxonomic views, the seed characters of *O. mammosa* and *O. sphegodes*, which are evaluated under the same species name and have been subject to taxonomic transfers under these names, clearly indicate two species that are morphologically distinct from each other. In the taxa of *O. sphegodes* found in Türkiye (ssp. *herae* and ssp. *caucasica*), the stigma cavity entrance at the base of the lip ranges from yellowish-green to orange or brick red; the lip varies from light to dark brown; the false eyes range from yellowish-green to black. On the other hand, in *O. mammosa*, the stigma cavity entrance at the base of the lip ranges from purplish to blackish; the lip ranges from purplish to blackish-purple; the false eyes are whitish-lilac to black. Additionally, *O. sphegodes* ssp. *herae* evaluated in the study, the flowers are smaller than those of *O. mammosa*.[30]

The priority of the name *O. sphegodes*, alongside its common morphological characteristics, has been a subject of discussion in some literature studies, leading to the publication of names that are mostly considered at the species level as subspecies of *O. sphegodes*. However, the seed morphological measurements do not support the taxonomic view previously published as that of *O. sphegodes* ssp. *mammosa* but rather indicate two clearly distinct taxa. In addition to the common character integrity within the genus *O. sphegodes*, the data obtained in this study have shed light on the taxonomic position of *O. lycia*. *O. lycia* is a highly localized endemic species specific to the Kaş district of Antalya (Türkiye). Recent detailed field studies conducted as part of conservation efforts have shown that its surface distribution is limited to four villages.[29] Considering the distributions of the species, stable taxonomic characters suggest that the species has transitional characters between *O. mammosa* and *O. argolica* and may be of hybrid origin. The data obtained from seed measurements indicate the closeness of the species to *O. sphegodes* compared to *O. mammosa* (Figure 3). Indeed, the recent literature shows that the name *O. lycia* is considered under *O. sphegodes* as *O. sphegodes* ssp. *lycia*.[37] When the taxonomy of the genus is evaluated, it is observed that color characters are as stable and dominant as structural characters. The floral covers and colors of *O. lycia* resemble those of *O. argolica*, while its pattern structure is similar to *O. sphegodes* and *O. mammosa*. No fragmentation is observed in the lips of the species, and there is no shoulder structure. The labelum, sepals, and petals are in shades of purplish-pink. Besides these characteristics observed in regional examples of *O. argolica*,

https://doi.org/10.1021/acsomega.4c03130
ACS Omega 2024, 9, 33773−33788

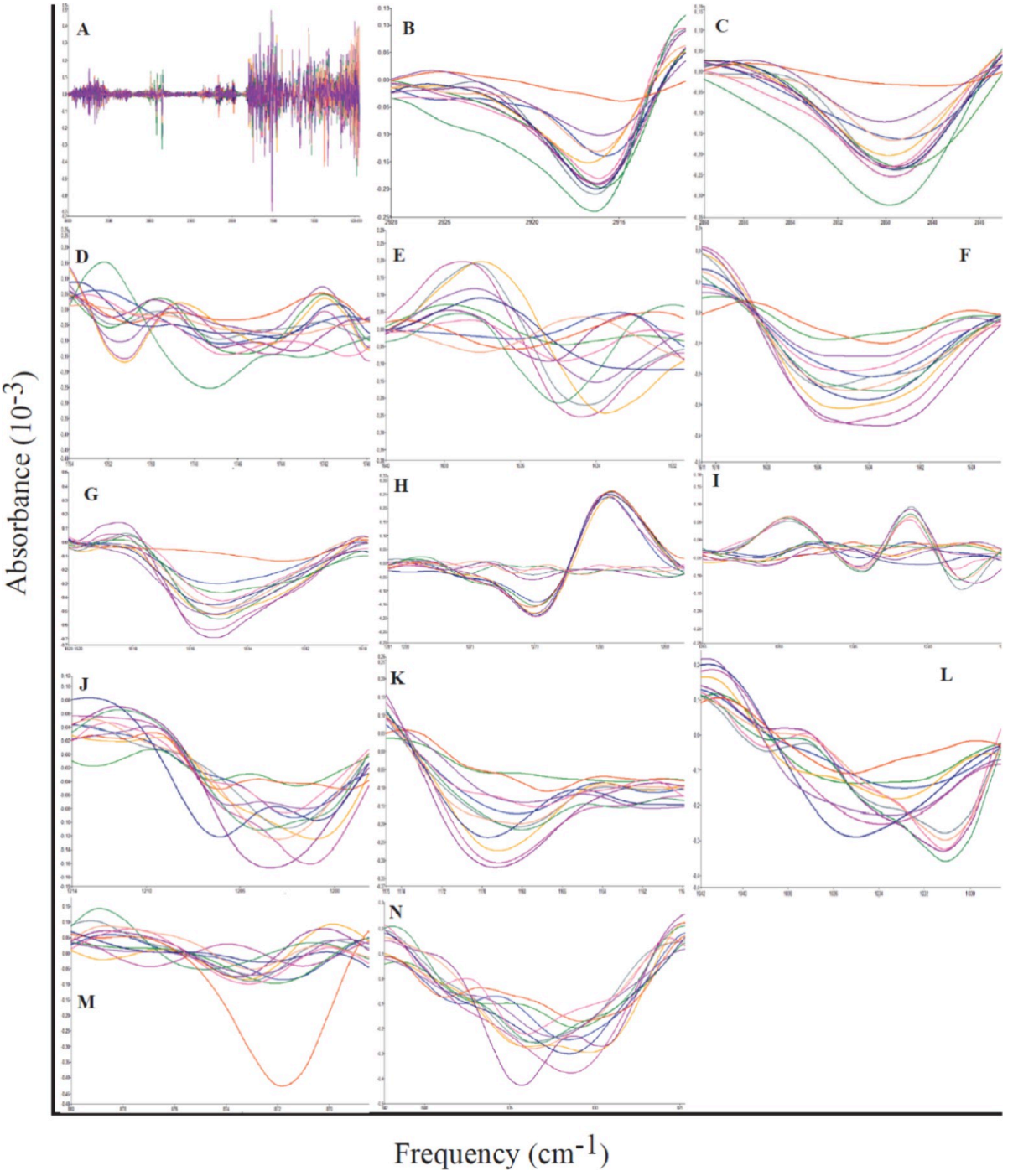

Figure 6. (A) Second derivative spectra of all samples with absorbance unit. (B) Detection of shifts in frequencies and determination of absorbance differences on the second derivative in the range of 2920−2915 cm^{-1}, (C) 2855−2848 cm^{-1}, (D) 1748−1740 cm^{-1}, (E) 1637−1630 cm^{-1}, (F) 1606−1602 cm^{-1}, (G) 1517−1513 cm^{-1}, (H) 1270−1260 cm^{-1}, (I) 1250−1240 cm^{-1}, (J) 1205−1200 cm^{-1}, (K) 1170−1160 cm^{-1}, (L) 1036−1032 cm^{-1}, (M) 875−870 cm^{-1}, (N) 836−830 cm^{-1}.

the pattern structure is in the shape of the letter H, as in *O. sphegodes* and *O. mammosa*. Additionally, in these two species, shades of yellowish-green dominate in the lips, sepals, and petals. Based on these morphological differences, the recent literature has published the name at the species level as *O. lycia*.[30]

These distinguishing characteristics are also supported by the morphological seed measurements obtained in the present study. The results of the FTIR analysis presented in this study also support the evaluation of *O. lycia* at the species level.

3.3. FTIR Analysis of Seed Coats. FTIR spectra of seedpods of 12 species belonging to the genus *Ophrys* are shown in Figure 5. The presence of various functional groups through the absorption bands of the phytocompounds of the seedpods is shown in Table 5.

Orchids are composed of many biochemical materials such as cellulose, hemicellulose, lignin, polysaccharides lipids, proteins, and other biofragments, which are visible at infrared spectra.[38] The observed peaks between the 3600 and 3100 cm^{-1} region are attributed to the characteristic peaks of O−H and C−H

https://doi.org/10.1021/acsomega.4c03130
ACS Omega 2024, 9, 33773−33788

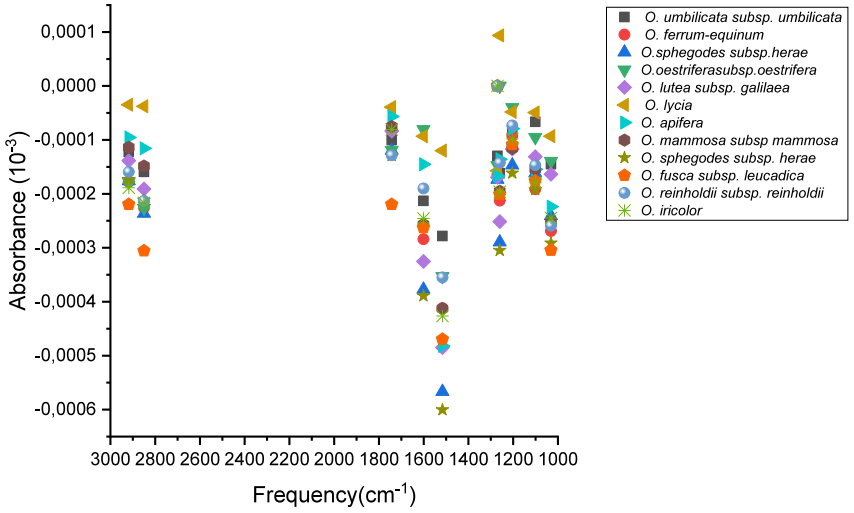

Figure 7. Absorbance values against some characteristic frequencies.

stretching vibrations.[39] Especially the broad peak at 3329 cm^{-1}, commonly found in every plant species, is labeled as the stretching vibration of hydroxyl groups in polysaccharides. This peak is essential evidence for inter- and intramolecular hydrogen bond vibration of cellulose and lignin in samples.[40,41] The vibrations found at 2917 and 2850 cm^{-1} belong to the asymmetrical and symmetrical $-CH_2$ stretching vibrations of aromatic methoxy groups and methylene and methyl groups in polysaccharides, lipids, and lignin compounds.[39,42] A weak peak at 1743 cm^{-1} is assigned to the unconjugated C═O stretching vibration of carboxyl and acetyl groups in hemicellulose moiety of samples.[40,43] Likewise vibration detected at 1639 cm^{-1} represents the C═O asymmetric vibration sourced from pectin, cellulose, and some alkaloids. At 1601, 1516, and 1443 cm^{-1}, observable peaks are labeled as aromatic skeleton vibration of lignin groups, COO− stretching of hemicellulose, and C−H plane deformation of celluloses.[44,45] The bands seen at 1371, 1318, and 1239 cm^{-1} are assigned as asymmetric CH_2 bending, CH_2 wagging, in plane OH bending of phenolic groups, and CH deformation, respectively.[46,47] The peak at 1155, 1102, and 1030 cm^{-1} are associated with C−O stretching of ester groups, aromatic C−H deformation of signal units, and O−H stretching of primary alcohols of cellulose and lignin.[48,49] The observable peak seen at 833 is labeled as C−H out-of-plane deformation of lignin groups.[11,50] All infrared bands and peaks are in good agreement with the literature studies.

In FTIR spectroscopy, secondary peaks refer to smaller or less prominent peaks observed in addition to the primary absorption peaks. These peaks can arise from various factors such as vibrations of side groups within the molecule, the presence of different functional groups, secondary interactions between molecules (e.g., hydrogen bonding), and the presence of additives or contaminants in the sample. Secondary peaks provide more detailed information about the molecular structure and accurately identifying these peaks aids in a better understanding of the molecule's chemical structure and interactions.[51] As stated in previous studies in the literature and this work, infrared spectroscopy has many purposes for usage in many scientific works.[52,53] One of the usages is finding the functional groups located in samples by detecting frequency values in the spectrum. Determination of functional groups gives essential information (i) about the chemical contents, (ii) about structural knowledge, and (iii) about the number of analytes by calculating peak areas. Likewise, infrared spectroscopy can prove the similarity of samples that are investigated. However, the number of chemical components in samples, such as plants such as orchids, causes the escalate the number of vibrations and makes the spectra more difficult to examine. In addition to this problem, some peaks that can give important evidence about structural, chemical, and quantitative information can be invisible in complex spectra. This problem can be solved by obtaining the second-order (derivative) spectrum from the zero-order spectrum.[54]

In this study, it is obviously clear that infrared spectra of all *Ophrys* genus are nearly the same because they have similar vibration frequencies. These data can give the idea that all investigated samples are of the same type, and structure and can contain the same amount of biomolecules. In response to this, when the second-order spectra of samples are examined, the observed differences in absorbance values at similar and several different frequency values indicate that the samples are different. These important differences in spectra are given in some regions with changes in frequency and absorbance in Figure 6.

Although the differences were figured out in second derivative spectra, due to the number of analyzed samples, spectra were converted to simple graphs to explain Figure 5 more clearly. For this purpose, the calculated absorbance values from second-order spectra can be used as a fingerprint for examining the differences and similarities in analyzed samples, as shown in Figures 7 and 8.

It is obviously seen that Figures 6 and 7 show and prove the variability in samples more explainable. From the two figures, it is observed clearly that *O. lycia* has almost different absorbance value for each frequency according to other species, which proves that *O. lycia* differs totally from other samples. When Figure 7 is analyzed in detail, it is seen that *O. oestrifera* subsp. *oestrifera* is a different species, but it may be close to *O. lycia*. *O. umblicata* subsp. *umblicata* is another sample that is distinguished clearly by its absorbance values at 1600−1000 cm^{-1}. *O. apifera* also has different absorbance values in the region 2950−1600 cm^{-1}. Although these data prove that this species may be different, the fact that the peaks in the fingerprint region are common with species *O. reinholdii* subsp. *reinholdii* show that these two species can be in the same type. The absorbances values in region 1500−1000 cm^{-1} are very close to each other for species *O. ferrum-equinum*, *O. mammosa* subsp.

https://doi.org/10.1021/acsomega.4c03130
ACS Omega 2024, 9, 33773−33788

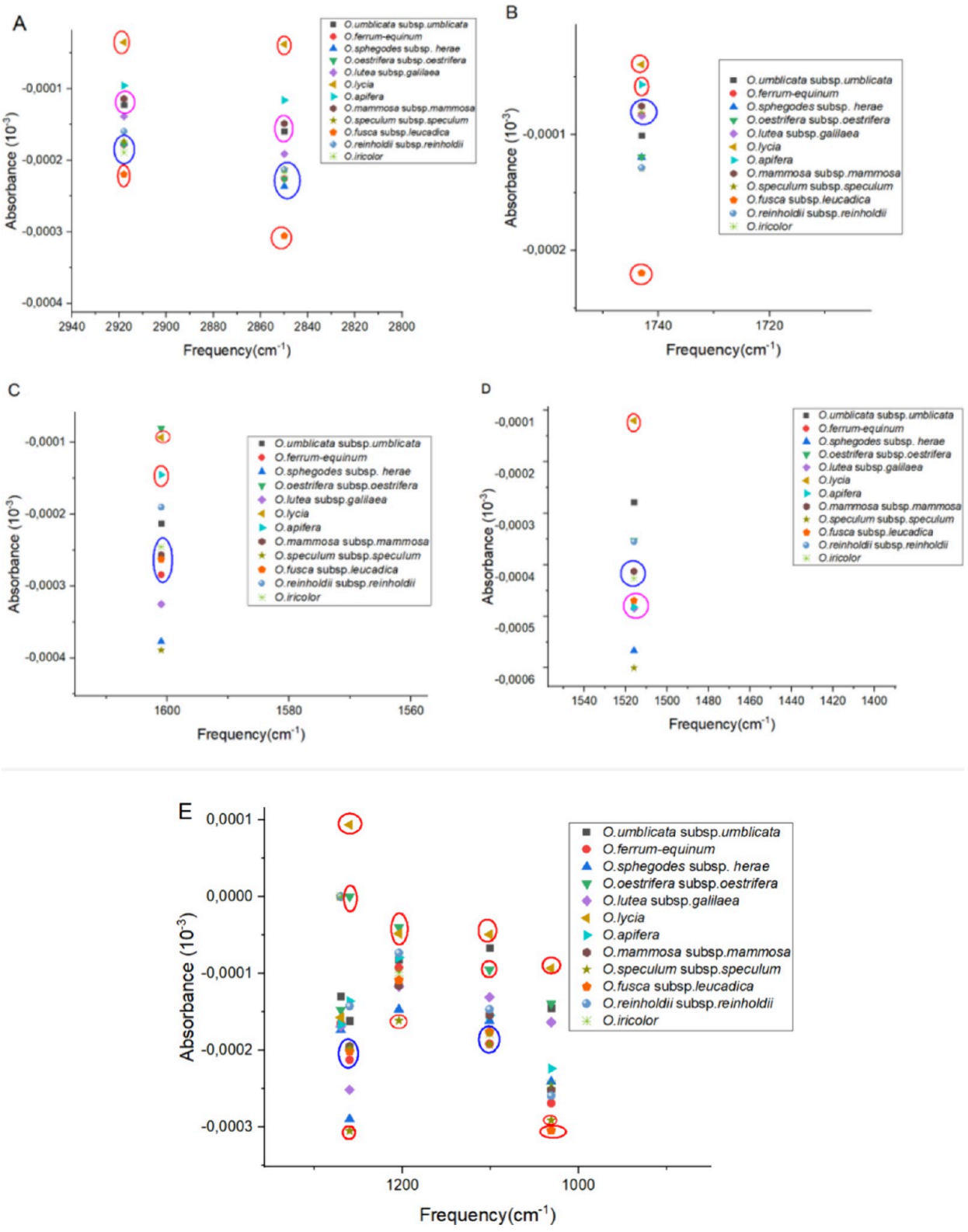

Figure 8. Absorbance values of all samples for (A) 2917 and 2850 cm^{-1}, (B) 1743 cm^{-1}, (C) 1601 cm^{-1}, (D) 1515 cm^{-1}, and (E) 1240, 1101, and 1031 cm^{-1}.

mammosa, *O. fusca* subsp. *leucadica*, *O. reinholdii* subsp. *reinholdii*, and *O. iricolor*, which may prove that these species are close to each other. Especially three species *O. ferrum-equinum*, *O. mammosa* subsp. *mammosa*, and *O. iricolor* have almost the same absorbance value for each investigated frequency. *Ophrys speculum* subsp. *speculum* has slightly different absorbance values from others makes it a different species. When all figures examined carefully, it was observed that *O. sphegodes* subsp. *herae* is one of the different species and can be a closer type with *O. speculum* subsp. *speculum*. Although *O. lutea* subsp. *galilaea* is considered to be in the same class as some species for

https://doi.org/10.1021/acsomega.4c03130
ACS Omega 2024, 9, 33773−33788

each frequency value, the small difference in absorption values indicates that this species may be in a separate class.

Fourier-transform infrared (FTIR) spectroscopy is a powerful analytical tool commonly used in the chemical analysis of biological materials. This method offers a fast, eco-friendly, and cost-effective option for examining plant chemical compositions.[55] When used in conjunction with leaf surface measurements, FTIR spectroscopy holds great promise for assisting in the identification of plants at the genus and (sub)species levels. This analytical method allows for the identification of major chemical groups and chemical bonds, providing information about the biochemical compounds present in the sample. Additionally, FTIR spectroscopy aids in the identification of the main organic components of plant materials and characterizes the inorganic compounds found in plants and soil.[56,57]

The results of our study show that especially the three species *O. ferrum-equinum*, *O. mammosa* subsp. *mammosa*, and *O. iricolor* have almost the same absorption values at each investigated frequency. Additionally, it is clearly observed that *O. lycia* has absorption values at each frequency that are almost different from those of the other species, proving that *O. lycia* is entirely different from the other samples. These data can be used in conjunction with morphological data for taxonomic character separation. FTIR spectroscopy has been successfully used in a series of studies aimed at distinguishing different species in plant biology. For example, it has been successfully used in studies on cell wall mutant plants,[58,59] cell wall composition and structure,[60] mechanical properties and molecular dynamics of plant cell wall polysaccharides,[61] and determination of fruit content in processed foods.[62] Recent studies have shown that FTIR has great taxonomic value at the species and subspecies levels in the *Hypericum* and *Triadenum* genera and reflects phylogenetic relationships among higher plant species.[63] In previous studies, Görgülü et al.[64] used FTIR to characterize and distinguish species in the *Acantholimon*, *Ranunculus*, and *Astragalus* genera, suggesting that FTIR could be used as a new method to distinguish plants at the genus level and even based on chemical structural differences. FTIR has also been successfully used to determine the level of species growing under different environmental conditions. In another study, Barsberg et al.[3] demonstrated that ATR-FT-IR spectroscopy can distinguish C-lignin from G/S-lignin, thus allowing for the monitoring of accumulations in orchid seed coats in the days following pollination. This method has particular value for the outer seed coat layer. Additionally, it can distinguish other molecular components in seed coats and demonstrate the varying seed coat chemistry among the species. The preference for C-lignin and the predicted linear extended polymer conformations suggest that the seed coat may form an optimal hydrophobic film or barrier in the interaction with lipid components. This is fundamentally different from the expected more complex amorphous polymers of G/S-lignin. This arrangement of C-lignin has been found to enhance the overall barrier properties and durability of the seed coat.

5. CONCLUSIONS

This study aimed to compare the morphometric and chemical contents of seeds from specific *Ophrys* species, examine interspecies relationships, and achieve specific objectives. The findings underscore the significant role of morphological and chemical analyses in taxonomic classification. Particularly, it highlights the inadequacy of relying solely on morphological characteristics to determine taxonomic positions and emphasizes the effectiveness of chemical analyses in revealing differences among species. Future studies should encompass a broader range of species, integrate genetic analyses, and explore ecological and physiological factors. This approach could lead to a deeper understanding of orchid seed biology and enable more precise taxonomic classification. Future research should broaden the scope to include a wider range of species, particularly endemic species and geographical variations. This could contribute to a better understanding of taxonomic diversity and the development of strategies for conservation of biodiversity conservation. Additionally, integrating genetic analyses can deepen the investigation of interspecies relationships and evolutionary connections, complementing morphological and chemical data in supporting taxonomic classification. Studies focusing on ecological and physiological factors are crucial for providing comprehensive insights into the life cycles, habitat preferences, and adaptations of orchids. This knowledge is essential for effectively directing conservation efforts and habitat restoration effectively. In conclusion, the findings of this study provide a solid foundation for further research on orchid seed biology and taxonomy. This foundation represents a significant step toward scientific advancements and contributions to the sustainability of natural ecosystems.

■ ASSOCIATED CONTENT

Data Availability Statement

Data will be made available on request.

■ AUTHOR INFORMATION

Corresponding Author

Erdi Can Aytar − *Faculty of Agriculture, Department of Horticulture, Usak University, Uşak 64900, Türkiye;* orcid.org/0000-0001-6045-0183; Email: erdi.aytar@usak.edu.tr

Authors

İsmail Gökhan Deniz − *Faculty of Science, Department of Biology, Akdeniz University, Antalya 07058, Türkiye*

Demet Incedere − *Faculty of Science, Department of Biology, Ondokuz Mayıs University, Samsun 55100, Türkiye*

Yasemin Özdener Kömpe − *Faculty of Science, Department of Biology, Ondokuz Mayıs University, Samsun 55100, Türkiye*

Taşkın Basılı − *Faculty of Science, Department of Chemistry, Ondokuz Mayıs University, Samsun 55139, Türkiye*

İnes Harzli − *Faculty of Science, Department of Biology, Ondokuz Mayıs University, Samsun 55100, Türkiye*

Alper Durmaz − *Ali Nihat Gokyigit Botanical Garden Application and Research Center, Artvin Coruh University, Artvin 08000, Türkiye*

Complete contact information is available at: https://pubs.acs.org/10.1021/acsomega.4c03130

Author Contributions

E.C.A., Y.Ö.K., and İ.G.D. conceived and designed the research. E.C.A., A.D., D.İ.U., and İ.H. set up the experiment and collected the data. E.C.A., T.B., and A.D. conducted the analyses and visualizations. All authors carefully reviewed the final version.

Notes

The authors declare no competing financial interest.

https://doi.org/10.1021/acsomega.4c03130
ACS Omega 2024, 9, 33773−33788

■ ACKNOWLEDGMENTS

We would like to express our gratitude to Uşak University for their support and contributions to this research.

■ REFERENCES

(1) Arditti, J.; Michaud, J. D.; Healey, P. L. Morphometry of orchıd seeds. i. paphıopedılum and natıve calıfornıa and related specıes of cyprıpedıum. *Am. J. Bot* **1979**, *66* (10), 1128−1137.
(2) Akçin, T. A.; Ozdener, Y.; Akçin, A. Taxonomic value of seed characters in orchids from Turkey. *Belgian J. Bot.* **2009**, 124−139.
(3) Barsberg, S. T.; Lee, Y. I.; Rasmussen, H. N. Development of C-Lignin with G/S-Lignin and Lipids in Orchid Seed Coats − an Unexpected Diversity Exposed by ATR-FT-IR Spectroscopy. *Seed Sci. Res.* **2018**, *28* (1), 41−51.
(4) Süngü Şeker, Ş. What Does the Quantitative Morphological Diversity of Starch Grains in Terrestrial Orchids Indicate? *Microsc Res. Tech* **2022**, *85* (8), 2931−2942.
(5) Rasmussen, H. N.; Dixon, K. W.; Jersáková, J.; Těšitelová, T. Germination and Seedling Establishment in Orchids: A Complex of Requirements. *Ann. Bot* **2015**, *116* (3), 391−402.
(6) Kodahl, N.; Johansen, B. B.; Rasmussen, F. N. The Embryo Sac of Vanilla Imperialis (Orchidaceae) Is Six-Nucleate, and Double Fertilization and Formation of Endosperm Are Not Observed. *Botanical Journal of the Linnean Society* **2015**, *177* (2), 202−213.
(7) Arditti, J.; Ghani, A. K. A. Tansley Review No. 110. Numerical and Physical Properties of Orchid Seeds and Their Biological Implications. *New Phytol* **2000**, *145* (3), 367−421.
(8) Healey, P. L.; Michaud, J. D.; Arditti, J. Morphometry of Orchid Seeds. Iii. Native California And Related Species Of Goodyera, Piperia, Platanthera And Spiranthes. *Am. J. Bot* **1980**, *67* (4), 508−518.
(9) Aybeke, M. Pollen and Seed Morphology of Some Ophrys L. (Orchidaceae) Taxa. *Journal of Plant Biology* **2007**, *50* (4), 387−395.
(10) Munir, M.; Ahmad, M.; Waseem, A.; Zafar, M.; Saeed, M.; Wakeel, A.; Nazish, M.; Sultana, S. Scanning Electron Microscopy Leads to Identification of Novel Nonedible Oil Seeds as Energy Crops. *Microsc Res. Tech* **2019**, *82* (7), 1165−1173.
(11) Barsberg, S. T.; Lee, Y. I.; Rasmussen, H. N. Development of C-Lignin with G/S-Lignin and Lipids in Orchid Seed Coats − an Unexpected Diversity Exposed by ATR-FT-IR Spectroscopy. *Seed Sci. Res.* **2018**, *28* (1), 41−51.
(12) Aytar, E. C.; Harzli, I.; Özdener Kömpe, Y. Phytochemical Analysis of Anacamptis Coriophora Plant Cultivated Using Ex Vitro Symbiotic Propagation. *Chem. Biodiversity* **2023**, *20* (12), No. e202301218.
(13) Brundrett, M. C.; Scade, A.; Batty, A. L.; Dixon, K. W.; Sivasithamparam, K. Development of in Situ and Ex Situ Seed Baiting Techniques to Detect Mycorrhizal Fungi from Terrestrial Orchid Habitats. *Mycol Res.* **2003**, *107* (10), 1210−1220.
(14) Batty, A. L.; Dixon, K. W.; Brundrett, M.; Sivasithamparam, K. Constraints to Symbiotic Germination of Terrestrial Orchid Seed in a Mediterranean Bushland. *New Phytologist* **2001**, *152* (3), 511−520.
(15) Skotti, E.; Pappas, C.; Kaiafa, M.; Lappa, I. K.; Tsitsigiannis, D. I.; Giotis, C.; Bouchagier, P.; Tarantilis, P. A. Discrimination and Quantification of Aflatoxins in Pistachia Vera Seeds Using FTIR-DRIFT Spectroscopy after Their Treatment by Greek Medicinal and Aromatic Plants Extracts. *Food Sci. Eng.* **2020**, *1*, 45−57.
(16) De Luca, M.; Terouzi, W.; Ioele, G.; Kzaiber, F.; Oussama, A.; Oliverio, F.; Tauler, R.; Ragno, G. Derivative FTIR Spectroscopy for Cluster Analysis and Classification of Morocco Olive Oils. *Food Chem.* **2011**, *124* (3), 1113−1118.
(17) Kayabaş, A.; Yildirim, E. New Approaches with ATR-FTIR, SEM, and Contact Angle Measurements in the Adaptation to Extreme Conditions of Some Endemic Gypsophila L. Taxa Growing in Gypsum Habitats. *Spectrochim Acta A Mol. Biomol Spectrosc* **2022**, *270*, No. 120843.
(18) Götz, A.; Nikzad-Langerodi, R.; Staedler, Y.; Bellaire, A.; Saukel, J. Apparent Penetration Depth in Attenuated Total Reflection Fourier-Transform Infrared (ATR-FTIR) Spectroscopy of Allium Cepa L. Epidermis and Cuticle. *Spectrochim Acta A Mol. Biomol Spectrosc* **2020**, *224*, No. 117460.
(19) Dogan, A.; Siyakus, G.; Severcan, F. FTIR Spectroscopic Characterization of Irradiated Hazelnut (Corylus Avellana L.). *Food Chem.* **2007**, *100* (3), 1106−1114.
(20) Baker, M. J.; Trevisan, lio; Bassan, P.; Bhargava, R.; Butler, H. J.; Dorling, K. M.; Fielden, P. R.; Fogarty, S. W.; Fullwood, N. J.; Heys, K. A.; Hughes, C.; Lasch, P.; Martin-Hirsch, P. L.; Obinaju, B.; Sockalingum, G. D.; Sul, J.; Strong, R. J.; Walsh, M. J.; Wood, B. R.; Gardner, P.; Martin, L. Using Fourier Transform IR Spectroscopy to Analyze Biological Materials. *Nat. Protocols* **2014**, *9*, 1771−1791.
(21) Durak, T.; Depciuch, J. Effect of Plant Sample Preparation and Measuring Methods on ATR-FTIR Spectra Results. *Environ. Exp Bot* **2020**, *169*, No. 103915.
(22) Liu, X.; Renard, C. M. G. C.; Bureau, S.; Le Bourvellec, C. Revisiting the Contribution of ATR-FTIR Spectroscopy to Characterize Plant Cell Wall Polysaccharides. *Carbohydr. Polym.* **2021**, *262*, No. 117935.
(23) Yeung, E. C. A Perspective on Orchid Seed and Protocorm Development. *Bot. Stud.* **2017**, *58* (1), 33.
(24) Kendon, J. P.; Rajaovelona, L.; Sandford, H.; Fang, R.; Bell, J.; Sarasan, V. Collecting near Mature and Immature Orchid Seeds for Ex Situ Conservation: 'In Vitro Collecting' as a Case Study. *Bot. Stud.* **2017**, *58* (1), 38.
(25) Kanlayavattanakul, M.; Pawakongbun, T.; Lourith, N. Dendrobium Orchid Polysaccharide Extract: Preparation, Characterization and in Vivo Skin Hydrating Efficacy. *Chin. Herb. Med.* **2019**, *11* (4), 400−405.
(26) Schiestl, F. P.; Peakall, R.; Mant, J. G.; Ibarra, F.; Schulz, C.; Franke, S.; Francke, W. The Chemistry of Sexual Deception in an Orchid-Wasp Pollination System. *Science* **2003**, *302* (5644), 437−438.
(27) Tsiftsis, S.; Tsiripidis, I. Temporal and Spatial Patterns of Orchid Species Distribution in Greece: Implications for Conservation. *Biodivers Conserv* **2020**, *29* (11−12), 3461−3489.
(28) Djordjević, V.; Tsiftsis, S.; Kindlmann, P.; Stevanović, V. Orchid Diversity along an Altitudinal Gradient in the Central Balkans. *Front Ecol Evol* **2022**, *10*, No. 929266.
(29) Gökhan DENİZ, İ.; Sümbül, H.; Sezik, E. A morphological investigation on non-apendix Ophrys L. Orchidaceae taxa in Antalya province. *Biol. Diversty Conversation* **2008**, *8* (1), 44−61.
(30) Kandemir, A.; Menemen, Y.; Yıldırım, H.; Aslan, S.; Ekşi, G.; Güner, I.; Çimen, A. Ö. (2014). *Resimli Türkiye Florası* (Vol. *1*). Güner, A. (Ed.). Alinihat Gökyiğit Vakfı.
(31) Prasongsom, S.; Thammasiri, K.; Pritchard, H. W. Seed Micromorphology and Ex Vitro Germination of Dendrobium Orchids. *Acta Hortic* **2017**, *1167*, 339−344.
(32) Gamarra, R.; Ortúñez, E.; Galán Cela, P.; Guadaño, V. Anacamptis versus Orchis (Orchidaceae): Seed Micromorphology and Its Taxonomic Significance. *Plant Syst. Evol.* **2012**, *298* (3), 597−607.
(33) Blunch, N. J.; Blunch, N. J.Introduction to Structural Equation Modeling Using IBM SPSS Statistics and Amos. 2012, 1−312.
(34) Lin, H.; Bean, S. R.; Tilley, M.; Peiris, K. H. S.; Brabec, D. Qualitative and Quantitative Analysis of Sorghum Grain Composition Including Protein and Tannins Using ATR-FTIR Spectroscopy. *Food Anal Methods* **2021**, *14* (2), 268−279.
(35) *Anales Del Jardin Botanico de Madrid*: 71, 2, 2014. Anales del Jardin Botanico de Madrid. - Semestrale = Six-monthly 2014, *71* (2), 1−55.
(36) Krishan, G.; Bhagwat, A.; Sejwal, P.; Yadav, B. K.; Kansal, M. L.; Bradley, A.; Singh, S.; Kumar, M.; Sharma, L. M.; Muste, M. Assessment of Groundwater Salinity Using Principal Component Analysis (PCA): A Case Study from Mewat (Nuh), Haryana, India. *Environ. Monit. Assess.* **2023**, *195* (137), 37.
(37) Kühn, R.; Pedersen, H.; Cribb, P.*Field Guide to the Orchids of Europe and the Mediterranean*. 2019.
(38) Zhao, D.; Han, C.; Tao, J.; Wang, J.; Hao, Z.; Geng, Q.; Du, B. Effects of Inflorescence Stem Structure and Cell Wall Components on the Mechanical Strength of Inflorescence Stem in Herbaceous Peony.

https://doi.org/10.1021/acsomega.4c03130
ACS Omega 2024, 9, 33773−33788

International Journal of Molecular Sciences **2012**, *13* (4), 4993−5009. *2012, Vol. 13, Pages 4993−5009*

(39) Hospodarova, V.; Singovszka, E.; Stevulova, N. Characterization of Cellulosic Fibers by FTIR Spectroscopy for Their Further Implementation to Building Materials. *Am. J. Anal. Chem.* **2018**, *9* (6), 303−310.

(40) Popescu, M. C.; Popescu, C. M.; Lisa, G.; Sakata, Y. Evaluation of Morphological and Chemical Aspects of Different Wood Species by Spectroscopy and Thermal Methods. *J. Mol. Struct.* **2011**, *988* (1−3), 65−72.

(41) Oh, S. Y.; Yoo, D. I.; Shin, Y.; Kim, H. C.; Kim, H. Y.; Chung, Y. S.; Park, W. H.; Youk, J. H. Crystalline Structure Analysis of Cellulose Treated with Sodium Hydroxide and Carbon Dioxide by Means of X-Ray Diffraction and FTIR Spectroscopy. *Carbohydr. Res.* **2005**, *340* (15), 2376−2391.

(42) Boeriu, C. G.; Bravo, D.; Gosselink, R. J. A.; Van Dam, J. E. G. Characterisation of Structure-Dependent Functional Properties of Lignin with Infrared Spectroscopy. *Ind. Crops Prod* **2004**, *20* (2), 205−218.

(43) Horikawa, Y.; Hirano, S.; Mihashi, A.; Kobayashi, Y.; Zhai, S.; Sugiyama, J. Prediction of Lignin Contents from Infrared Spectroscopy: Chemical Digestion and Lignin/Biomass Ratios of Cryptomeria Japonica. *Appl. Biochem. Biotechnol.* **2019**, *188* (4), 1066−1076.

(44) Sammons, R. J.; Harper, D. P.; Labbé, N.; Bozell, J. J.; Elder, T.; Rials, T. G. Characterization of Organosolv Lignins Using Thermal and FT-IR Spectroscopic Analysis. *BioResources* **2013**, *8* (2), 2752−2767.

(45) Poletto, M.; Pistor, V.; Zeni, M.; Zattera, A. J. Crystalline Properties and Decomposition Kinetics of Cellulose Fibers in Wood Pulp Obtained by Two Pulping Processes. *Polym. Degrad. Stab.* **2011**, *96* (4), 679−685.

(46) Rashid, T.; Kait, C. F.; Murugesan, T. A "Fourier Transformed Infrared" Compound Study of Lignin Recovered from a Formic Acid Process. *Procedia Eng.* **2016**, *148*, 1312−1319.

(47) Kline, L. M.; Hayes, D. G.; Womac, A. R.; Labbé, N. Simplified Determination of Lignin Content in Hard and Soft Woods via Uv-Spectrophotometric Analysis of Biomass Dissolved in Ionic Liquids. *BioResources* **2010**, *5* (3), 1366−1383. 2010, undefined

(48) Faix, O. Classification of Lignins from Different Botanical Origins by FT-IR Spectroscopy. *Holzforschung* **1991**, *45* (s1), 21−28.

(49) Hong, T.; Yin, J. Y.; Nie, S. P.; Xie, M. Y. Applications of Infrared Spectroscopy in Polysaccharide Structural Analysis: Progress, Challenge and Perspective. *Food Chem. X* **2021**, *12*, No. 100168.

(50) Fackler, K.; Stevanic, J. S.; Ters, T.; Hinterstoisser, B.; Schwanninger, M.; Salmén, L. FT-IR Imaging Microscopy to Localise and Characterise Simultaneous and Selective White-Rot Decay within Spruce Wood Cells. *Holzforschung* **2011**, *65* (3), 411−420.

(51) Kumosinski, T. F.; Farrell, H. M. Determination of the Global Secondary Structure of Proteins by Fourier Transform Infrared (FTIR) Spectroscopy. *Trends Food Sci. Technol.* **1993**, *4* (6), 169−175.

(52) Chylińska, M.; Szymańska-Chargot, M.; Zdunek, A. FT-IR and FT-Raman Characterization of Non-Cellulosic Polysaccharides Fractions Isolated from Plant Cell Wall. *Carbohydr. Polym.* **2016**, *154*, 48−54.

(53) Kacuráková, M.; Capek, P.; Sasinková, V.; Wellner, N.; Ebringerová, A. FT-IR Study of Plant Cell Wall Model Compounds: Pectic Polysaccharides and Hemicelluloses. *Carbohydr. Polym.* **2000**, *43* (2), 195−203.

(54) Acemi, A. Polymerization Degree of Chitosan Affects Structural and Compositional Changes in the Cell Walls, Membrane Lipids, and Proteins in the Leaves of Ipomoea Purpurea: An FT-IR Spectroscopy Study. *Int. J. Biol. Macromol.* **2020**, *162*, 715−722.

(55) Kayabaş, A.; Yildirim, E. New Approaches with ATR-FTIR, SEM, and Contact Angle Measurements in the Adaptation to Extreme Conditions of Some Endemic Gypsophila L. Taxa Growing in Gypsum Habitats. *Spectrochim Acta A Mol. Biomol Spectrosc* **2022**, *270*, No. 120843.

(56) von Aulock, F. W.; Kennedy, B. M.; Schipper, C. I.; Castro, J. M.; E. Martin, D.; Oze, C.; Watkins, J. M.; Wallace, P. J.; Puskar, L.; Bégué, F.; Nichols, A. R. L.; Tuffen, H. Advances in Fourier Transform Infrared Spectroscopy of Natural Glasses: From Sample Preparation to Data Analysis. *Lithos* **2014**, *206−207* (1), 52−64.

(57) Muhammad, S.; Wuyts, K.; Nuyts, G.; De Wael, K.; Samson, R. Characterization of Epicuticular Wax Structures on Leaves of Urban Plant Species and Its Association with Leaf Wettability. *Urban For Urban Green* **2020**, *47*, No. 126557.

(58) Chen, L.; Carpita, N. C.; Reiter, W. D.; Wilson, R. H.; Jeffries, C.; McCann, M. C. A Rapid Method to Screen for Cell-Wall Mutants Using Discriminant Analysis of Fourier Transform Infrared Spectra. *Plant Journal* **1998**, *16* (3), 385−392.

(59) Stewart, D.; Yahiaoui, N.; McDougall, G. J.; Myton, K.; Marque, C.; Boudet, A. M.; Haigh, J. Fourier-Transform Infrared and Raman Spectroscopic Evidence for the Incorporation of Cinnamaldehydes into the Lignin of Transgenic Tobacco (Nicotiana Tabacum L.) Plants with Reduced Expression of Cinnamyl Alcohol Dehydrogenase. *Planta* **1997**, *201* (3), 311−318.

(60) McCann, M. C.; Chen, L.; Roberts, K.; Kemsley, E. K.; Sene, C.; Carpita, N. C.; Stacey, N. J.; Wilson, R. H. Infrared Microspectroscopy: Sampling Heterogeneity in Plant Cell Wall Composition and Architecture. *Physiol. Plant.* **1997**, *100* (3), 729−738.

(61) Wilson, R. H.; Smith, A. C.; Kacurakova, M.; Saunders, P. K.; Wellner, N.; Waldron, K. W. The Mechanical Properties and Molecular Dynamics of Plant Cell Wall Polysaccharides Studied by Fourier-Transform Infrared Spectroscopy. *Plant Physiol* **2000**, *124* (1), 397−406.

(62) Wilson, R. H.; Slack, P. T.; Appleton, G. P.; Sun, L.; Belton, P. S. Determination of the Fruit Content of Jam Using Fourier Transform Infrared Spectroscopy. *Food Chem.* **1993**, *47* (3), 303−308.

(63) Kim, S. W.; Ban, S. H.; Chung, H.; Cho, S.; Chung, H. J.; Choi, P. S.; Yoo, O. J.; Liu, J. R. Taxonomic Discrimination of Flowering Plants by Multivariate Analysis of Fourier Transform Infrared Spectroscopy Data. *Plant Cell Rep* **2004**, *23* (4), 246−250.

(64) Gorgulu, S. T.; Dogan, M.; Severcan, F. The Characterization and Differentiation of Higher Plants by Fourier Transform Infrared Spectroscopy. *Appl. Spectrosc.* **2007**, *61* (3), 300−308. *Vol. 61, Issue 3, pp. 300−308*

https://doi.org/10.1021/acsomega.4c03130
ACS Omega 2024, 9, 33773−33788